

Online Research @ Cardiff

This is an Open Access document downloaded from ORCA, Cardiff University's institutional repository: <https://orca.cardiff.ac.uk/id/eprint/85072/>

This is the author's version of a work that was submitted to / accepted for publication.

Citation for final published version:

Moffa Sanchez, Paola, Born, Andreas, Hall, Ian R. ORCID: <https://orcid.org/0000-0001-6960-1419>, Thornalley, David J.R. and Barker, Stephen ORCID: <https://orcid.org/0000-0001-7870-6431> 2014. Solar forcing of North Atlantic surface temperature and salinity over the past millennium. Nature Geoscience 7 , pp. 275-278. 10.1038/ngeo2094 file

Publishers page: <http://dx.doi.org/10.1038/ngeo2094>
<<http://dx.doi.org/10.1038/ngeo2094>>

Please note:

Changes made as a result of publishing processes such as copy-editing, formatting and page numbers may not be reflected in this version. For the definitive version of this publication, please refer to the published source. You are advised to consult the publisher's version if you wish to cite this paper.

This version is being made available in accordance with publisher policies.

See

<http://orca.cf.ac.uk/policies.html> for usage policies. Copyright and moral rights for publications made available in ORCA are retained by the copyright holders.



Solar forcing of North Atlantic surface temperature and salinity over the last millennium

Paola Moffa-Sánchez^{1*}, Andreas Born^{2,3}, Ian R. Hall¹, David J.R. Thornalley^{1,4}, Stephen Barker¹

¹School of Earth and Ocean Sciences, Cardiff University, Cardiff, U.K.

²Oeschger Centre for Climate Change Research, Institute of Physics, University of Bern, Switzerland.

³Climate and Environmental Physics, Physics Institute, University of Bern, Bern, Switzerland

⁴Now at Department of Geography, University College London, London, U.K.

*To whom correspondence should be addressed. E-mail: MoffaSanchezPL@cardiff.ac.uk

During the last millennium, climate in the North Atlantic region has been characterised by variations, which, despite their small magnitude, had important societal impacts¹. The most favoured explanations for this variability invoke external forcing related to variable solar activity and explosive volcanism, with changes amplified by ocean and atmosphere feedbacks, mainly involving the Atlantic Meridional Overturning Circulation and the North Atlantic Oscillation². However, the scarcity of highly resolved archives has hampered our understanding of the role that ocean-atmosphere interactions played in these climate oscillations. Here, results from a sub-decadally resolved marine sediment core show multidecadal to centennial-scale abrupt changes in the properties of the upper limb of the Atlantic Meridional Overturning Circulation between 818-1780 years AD. These fluctuations present a strong correlation with solar irradiance variability. Model simulations support this finding and reveal that these hydrographic changes likely resulted from variability in the strength of the Subpolar Gyre driven by the frequency and persistence of atmospheric blocking events in the eastern North Atlantic as a response to solar irradiance variability. This coupled ocean-atmosphere response to solar irradiance minima may have contributed towards the consecutive cold winters documented in Europe during the Little Ice Age (1450-1850 years AD).

32 The import of salt to higher latitudes by the North Atlantic Current (NAC) is essential for
33 maintaining the high density of surface waters in the Nordic and Labrador Seas^{3,4}, a pre-
34 requisite for deep water formation. Deepwater formation is critical for the Atlantic
35 Meridional Overturning Circulation (AMOC) and therefore of great importance to the climate
36 system. Additionally, the heat released from the NAC, aided by the westerly winds,
37 contributes to ameliorating the climate of Europe⁵. Because of its large heat capacity, the
38 ocean is expected to be amongst the most predictable components of the climate system at
39 multidecadal time-scales. It is therefore of paramount importance to study past variability in
40 the properties of the NAC beyond the instrumental record to better constrain natural ocean
41 variability and its potential impacts on regional and global future climate.

42

43 To investigate multidecadal hydrographic variability of the NAC during the last millennium,
44 we use marine sediment core RAPID-17-5P (61° 28.90'N, 19° 32.16'W, 2303 m water depth;
45 Fig. 1) recovered from the Iceland Basin. The upper 600 m of the water column at the
46 core-site are dominated by the northward flowing NAC³. Temperature and salinity
47 reconstructions were produced by analysing paired Mg/Ca- $\delta^{18}\text{O}$ signals in the shells of the
48 planktonic foraminifera *Globorotalia inflata* (Supplementary Methods). The concentration of
49 Mg in calcite foraminiferal tests is an established proxy for temperature⁶, which combined
50 with the $\delta^{18}\text{O}$ composition of the same calcite, allows the isolation of the $\delta^{18}\text{O}$ of seawater
51 ($\delta^{18}\text{O}_{\text{sw}}$) and the estimation of salinity. *G. inflata* lives close to the base of the seasonal
52 thermocline⁷ and, due to the limited seasonal variation at this depth, it principally records
53 mean annual temperatures⁸. The chronology for RAPID-17-5P was obtained using 12 AMS
54 radiocarbon dates, which yielded a linear sedimentation rate of 0.16 cm/year, providing an
55 integrated sample resolution of ~6 years between 818-1780 years AD (Supplementary
56 Methods).

57 Our results reveal abrupt multidecadal to centennial shifts in the temperature and salinity of
58 the NAC waters of $\sim 3.5 \pm 1.1^\circ\text{C}$ and $\sim 1.2 \pm 0.8$ psu during the last millennium (Figure 2b,c).
59 The magnitude of the hydrographic variability is substantial and comparable to that recorded
60 in a lower resolution record spanning the present interglacial from a nearby site⁹ which
61 highlights the similarities in the ocean variability on a diverse range of time-scales. The
62 timing of the hydrographic shifts show a strong correlation with Total Solar Irradiance (TSI)
63 variability¹⁰ (Figure 2d). Periods of solar minima (maxima) generally correspond to cold and
64 fresh (warm and salty) conditions in the NAC (Figure 2). A Pearson's correlation coefficient
65 of 0.51 (n=77) with 95% confidence interval [0.31; 0.67] was estimated when correlating
66 temperature and TSI records, following Gaussian-interpolation to a common time-step of
67 ~ 12 -years (the minimum resolution of the temperature record) (Figure S3).

68

69 Wavelet transform analysis of the temperature record shows a clear 200-year cycle with
70 enhanced power between 1200-1650 years AD (Figure S5). In addition, cross-spectral
71 analysis shows that temperature and TSI are coherent above the 90% confidence level in the
72 frequency range 177-227 years (Figure S4). This variance is similar to deVries solar activity
73 cycles (~ 210 years) and supports the correlation found between the NAC temperature and
74 TSI records over the last millennium.

75

76 To investigate the feedback processes linking TSI variability and the recorded abrupt ocean
77 changes we analysed climate model simulations performed using Community Climate
78 System Model version 4.0 (CCSM4), forced with TSI variability and volcanic aerosols for
79 the last millennium (850-1850 years AD)¹¹. The modelling results also present a strong
80 positive correlation between temperature and salinity south of Iceland and solar irradiance
81 (Figure 3a,b), although the hydrographic variability in the model is of smaller amplitude than

82 in the proxy data. The highest correlations are found in the pathway of the NAC and
83 particularly in the path of its western branch, the Irminger Current. Additional temperature
84 and salinity proxy reconstructions of the Irminger Current, from a sediment core south of
85 Greenland (RAPiD-35-25B - Figure 1), show broad similarities with the results from RAPiD-
86 17-5P (Figure S6-S8), which confirm the westward propagation of the anomalies within the
87 warm Atlantic waters via the Irminger Current found in the model (Figure 3a,b).

88

89 The similar timing of volcanic eruptions and solar minima during the last millennium (Figure
90 2a-b) makes the separation of their relative climatic influence difficult and has been the
91 subject of much debate in recent literature. For instance, the injection of aerosols into the
92 stratosphere by volcanic activity may have additionally contributed towards the cold fresh
93 events recorded south of Iceland (Figure 2a-c)^{e.g. 12}. In this study, decomposition of the
94 relative contribution of the solar and volcanic forcing to the ocean changes was explored by
95 performing a series of sensitivity tests in CCSM4. In these experiments we find that changes
96 in volcanic forcing yield a qualitatively different dynamic response of the atmosphere-ocean
97 system in our region of study compared to solar forcing which consistently explain the key
98 changes described in the transient simulation (Figure S11-S13). We therefore conclude that
99 solar irradiance was the dominant forcing on the centennial-scale ocean changes.

100

101 The NAC and its north-western branch, the Irminger Current, constitute the main boundary
102 currents of the Subpolar Gyre (SPG) (Figure 1). Changes in the strength of the SPG therefore
103 influence the properties, structure and volume transport of the surface circulation in the North
104 Atlantic¹³. Previous modelling and palaeodata studies have interpreted changes in the
105 hydrographic properties of the NAC, and particularly salinity south of Iceland, to be
106 controlled by frontal mixing resulting from changes in the spatial extent of the SPG as a

107 response to changes in its strength^{9,13}. For example, during a weak and contracted SPG
108 circulation a displacement of the Subpolar Front to the west would increase the contribution
109 of subtropical versus subpolar waters to the NAC, making it warm and salty. In this study,
110 however, volume transport analysis of the SPG in CCSM4 over the last millennium indicate
111 that warmer and saltier conditions found south of Iceland and in the pathway of the Irminger
112 Current correspond to periods of stronger SPG circulation (Figure 3c). This is in agreement
113 with recent observations that show advection may play a dominant role in determining the
114 properties of water masses along the Irminger Current¹⁴ (Supplementary Discussion). An
115 increase in the heat and particularly salt transport by the IC into the Labrador Sea may have
116 additionally promoted deep convection in this region⁴, potentially impacting the AMOC.

117

118 Since ocean gyres are largely driven by wind-stress forcing, changes in the SPG strength and
119 NAC properties found in the proxy and model results are likely linked to shifts in
120 atmospheric circulation. The North Atlantic Oscillation (NAO) is the dominant mode of
121 atmospheric variability in the North Atlantic¹⁵. During a positive NAO state the increase in
122 the strength of the westerlies promotes surface heat loss and ultimately leads to deeper
123 convection in the Labrador Sea, baroclinically driving a stronger SPG. However, an emergent
124 view derived from both model and observational data is that small-scale atmospheric patterns
125 in the Northeast Atlantic, such as atmospheric blocking events as part of the East Atlantic
126 Pattern or polar mesoscale storms, may contribute considerably to driving North Atlantic
127 surface circulation¹⁶⁻¹⁸.

128

129 Atmospheric blocking events are mid-latitude weather systems where a quasi-stationary high
130 pressure system located in the Northeast Atlantic modifies the flow of the westerly winds by
131 blocking or diverting their pathway. Blocking events derive from instabilities of the jet

132 stream and predominantly develop in winter, typically in association with a negative NAO¹⁹.
133 The impacts of the frequency and magnitude of these small-scale atmospheric systems are not
134 restricted to the ocean¹⁶⁻¹⁸ but also have important effects on European temperatures, as they
135 block the meridional transport of warm maritime winds (which are replaced by the cold
136 north-easterlies). For example, Atlantic blocking events are thought to have been responsible
137 for several recent cold European winters (i.e. 1963, 2009, 2010 and 2013).

138

139 The analysis of Sea Level Pressure (SLP) patterns in our CCSM4 simulation reveals the
140 presence of an anomalous high-pressure system off West Europe during periods of solar
141 minima (Figure 4), which correspond to a weaker SPG (Figure 3c) and a colder and fresher
142 NAC (Figure 2 and 3a,b). This finding is in line with recent studies that suggest a decrease in
143 SPG strength with more frequent and stronger atmospheric blocking events on decadal time-
144 scales^{16,18}. The results agree with the early concept that the severe winters experienced in
145 Europe during the Maunder Minimum were caused by periods of increased atmospheric
146 blocking¹ and are also consistent with SLP field reconstructions which show a high pressure
147 system over North-west Europe towards the end of the Spörer and during the Maunder
148 Minimum²⁰. Similarly, a number of studies suggest a negative NAO state during the Maunder
149 Minimum or other periods of low TSI²¹, in agreement with increased blocking arising from
150 the weaker westerly winds.

151

152 Growing evidence for the linkage between solar variability and frequency of blocking in the
153 Northeast Atlantic has also been provided by meteorological studies. Modern observations
154 show strong solar modulation of the blocking frequency and positioning during the 11-year
155 solar cycles for the last 50 years, impacting substantially on UK winter temperatures^{22,23}.

156 Periods of solar minima, such as the Maunder Minimum, have also been shown to correspond

157 to cold temperatures in the Central England Temperature record, which is dominated by the
158 frequency of winter blockings²⁴. The regional atmospheric response to solar forcing has often
159 been explained through variability in stratospheric temperatures as the response of ozone
160 formation to changes in ultra violet radiation^{21,22,25}. Changes in stratospheric temperatures
161 have a top-down effect on tropospheric dynamics and hence induce variability of the jet
162 stream^{22,26}. Nonetheless, modelling studies with a simplified representation of the upper
163 atmosphere, like CCSM4, find a similar response to solar forcing suggesting that other
164 feedbacks such as ocean feedbacks on the atmosphere, internal climate dynamics and Pacific
165 teleconnections may also be influential²¹. On decadal time-scales, modelling and
166 observational studies have previously identified separate relationships between solar
167 irradiance and Atlantic blocking events^{22,23,26} and blocking events and SPG strength^{16,18}
168 individually. Our findings support a direct linkage between these three components of the
169 Earth's climate system, which probably shaped the North Atlantic climate over the last
170 millennium.

171
172 Climate variability on decadal timescales is largely believed to be dominated by internal
173 processes rather than external forcing, which presents large difficulties for much-needed
174 climate projections of the coming decades. However, the proxy evidence presented here,
175 supported by model results, suggest that external forcing by solar variability has a
176 considerable impact on multidecadal-centennial ocean-atmospheric dynamics, with important
177 effects on regional climate such as European winters. In this context, predictions of a
178 forthcoming prolonged period of low solar activity²⁷ imply direct climatic consequences.

179
180 Despite the hemispheric temperature changes expected from solar minima being much
181 smaller than the warming from future CO₂ emissions, regional climate variability associated

182 with solar-induced ocean-atmosphere feedbacks could be substantial and should be taken into
183 consideration when projecting future climate changes.

184

185 **Methods Summary**

186 Paired $\delta^{18}\text{O}$ and Mg/Ca analyses were performed on 6-20 *Globorotalia inflata* (300-355 μm)
187 tests. Samples were prepared using the method outlined by ref.28 and analysed using a
188 Finnigan Element XR high-resolution inductively coupled plasma mass spectrometer (Cardiff
189 University). Calculation of average shell weights and investigation of the co-variability of
190 Mg/Ca record to metals such as Fe, Mn and Al shows that no secondary effects such as
191 partial dissolution or trace metal contamination have altered the primary temperature signal in
192 the Mg/Ca record. Mg/Ca values were converted to calcification temperatures using $\text{Mg/Ca} =$
193 $0.675 \exp(0.1xT)$ after the core-top calibration by ref.⁹. Stable isotope measurements were
194 carried out on a Thermo Finnigan MAT 252 isotope ratio mass spectrometer coupled to a
195 Kiel II carbonate preparation device at Cardiff University. For more details see
196 Supplementary Methods.

197

198 **Additional information**

199 Correspondence and requests for materials should be addressed to P.M.

200

201

202 **Acknowledgements**

203 We are grateful to Julia Becker and Anabel Morte-Ródenas for laboratory assistance and
204 thank Nick McCave and the crew of *RV Charles Darwin 159* for their assistance with sample
205 collection. We also thank Christoph C. Raible for useful discussions and Carl-Friedrich
206 Schleussner for early discussions on the subject. This work was supported by funding from
207 the U.K. National Environmental Research Council (NERC). Computing resources were
208 provided by NCAR's Computational and Information Systems Laboratory (CISL) sponsored

209 by the National Science Foundation and other agencies. A.B. is supported by the European
210 Commission under the Marie Curie Intra-European Fellowship ECLIPS (PIEF-GA-2011-
211 300544) and the 'National Centre for Excellence in Research: Climate' of the Swiss National
212 Science Foundation. P.M. and I.H. also gratefully acknowledge the support of the Climate
213 Change Consortium of Wales (www.c3wales.org).

214

215 **Author contribution**

216 P.M. sampled the core, processed the samples, performed the measurements, data analysis
217 and interpretation; A.B. performed the model analysis and interpretation. I.R.H, D.J.R.T. and
218 S.B. supervised P.M. during her PhD; I.R.H. and D.J.R.T. participated in the retrieval of the
219 sediment core material and initiated the project; All authors contributed towards the writing
220 of the manuscript.

Figure captions

Figure 1

Figure 1. Sea surface temperature map for January 2008 showing the schematic surface circulation of the North Atlantic and the core location of RAPiD-17-5P and RAPiD-35-25B (Supp. Material). Solid arrows indicate the warm salty waters from the tropics, namely the NAC and its main branches such as the Irminger Current (IC). The dashed lines indicate the cold polar south-flowing waters such as the East Greenland Current, West Greenland Current and Labrador Current which constitute the Western branch of the SPG. Location of RAPiD-17-5P (61° 28.90'N, 19° 32.16'W, 2303m water depth) and RAPiD-35-25B (57° 30.47'N, 48° 43.40'W, 3486 m water depth) are marked with a black circle (adapted from UK-Met office OSTIA data²⁹).

Figure 2

Proxy records from RAPiD-17-5P. (a) Solar irradiance forcing reconstruction based on the cosmogenic nuclide ^{10}Be ¹⁰ (orange) and global volcanic stratospheric aerosols³⁰ (grey). **(b)** Temperature and **(c)** salinity/ $\delta^{18}\text{O}_{\text{sw}}$ estimates derived from paired Mg/Ca and $\delta^{18}\text{O}$ measurements in *G. inflata* calcite from RAPiD-17-5P. **(d)** Three-point smoothed

temperature record from RAPiD-17-5P (black) and ΔTSI^{10} (orange). A 12.42 year lag has been imposed on the ΔTSI forcing as indicated from the highest Pearson Correlation (Supplementary notes, Figure S2). Shaded areas highlight the well-known periods of solar minima.

Figure 3

Modelling results from CCSM4. Pointwise correlation of TSI with (a) temperature and (b) salinity averaged between 150-204 m water depth. (c) Regression of TSI with the depth-integrated stream function (all time-series were filtered with a 50 year low-pass filter). Black contours show the time-average depth-integrated stream function and areas with correlations above 95% confidence threshold are dotted. Negative values indicate stronger anti-clockwise circulation. The location of RAPiD-17-5P is marked with a black circle.

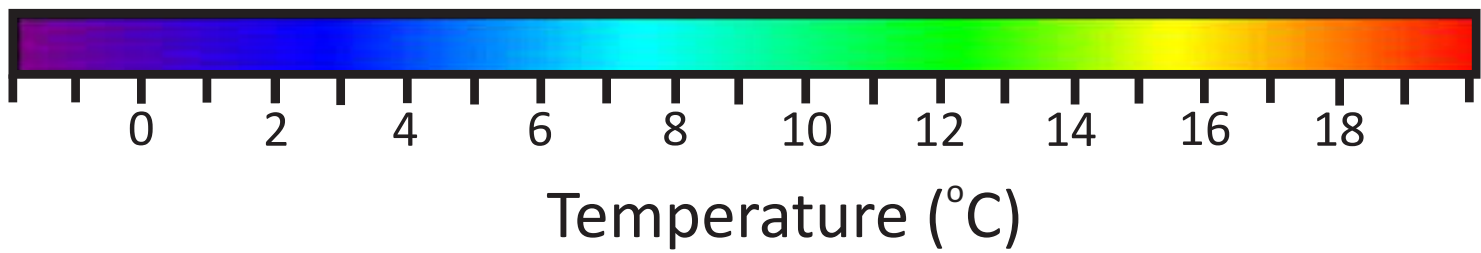
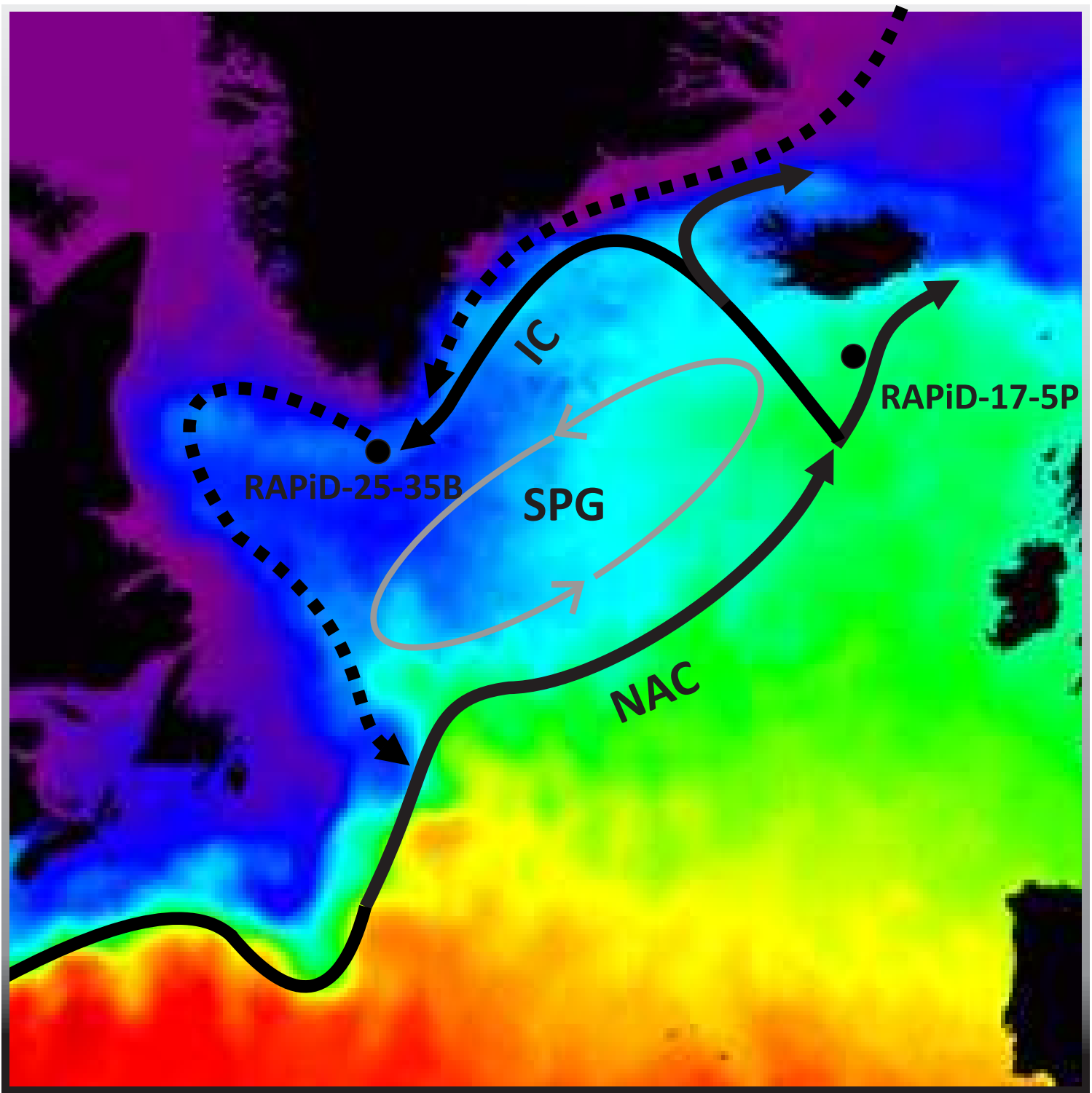
Figure 4

Atmospheric changes in CCSM4. Differences in sea level pressure of weak-strong TSI composites ($\pm 1\sigma$) in CCSM4 reveals an anomalous high pressure system during low TSI over the British Isles and the eastern North Atlantic, indicative of increased winter blocking. Time-series have been filtered with a 50 year low-pass filter (See Figure S14 for a SLP regression plot).

References

1. Lamb, H. . Climatic variation and changes in the wind and ocean circulation: The Little Ice Age in the northeast Atlantic. *Quat. Res.* 11, 1–20 (1979).
2. Trouet, V. *et al.* Persistent positive north atlantic oscillation mode dominated the medieval climate anomaly. *Science* 324, 78–80 (2009).
3. Østerhus, S., Turrell, W. R., Jónsson, S. & Hansen, B. Measured volume, heat, and salt fluxes from the Atlantic to the Arctic Mediterranean. *Geophys. Res. Lett.* 32, L07603 (2005).
4. Straneo, F. Heat and freshwater transport through the central Labrador Sea. *J. Phys. Oceanogr.* 36, 606–628 (2006).
5. Seager, R. *et al.* Is the Gulf Stream responsible for Europe’s mild winters? *Q. J. R. Meteorol. Soc.* 128, 2563–2586 (2002).
6. Elderfield, H. & Ganssen, G. Past temperature and $\delta^{18}\text{O}$ of surface ocean waters inferred from foraminiferal Mg/Ca ratios. *Nature* 405, 442–445 (2000).
7. Cléroux, C. *et al.* Mg/Ca and Sr/Ca ratios in planktonic foraminifera: Proxies for upper water column temperature reconstruction. *Paleoceanography* 23, PA3214 (2008).
8. Ganssen, G. M. & Kroon, D. The isotopic signature of planktonic foraminifera from NE Atlantic surface sediments: implications for the reconstruction of past oceanic conditions. *J Geol Soc Lond* 157, 693–699 (2000).
9. Thornalley, D. J. R., Elderfield, H. & McCave, I. N. Holocene oscillations in temperature and salinity of the surface subpolar North Atlantic. *Nature* 457, 711–714 (2009).
10. Steinhilber, F., Beer, J. & Fröhlich, C. Total solar irradiance during the Holocene. *Geophys. Res. Lett.* 36, L19704 (2009).
11. Landrum, L. *et al.* Last Millennium Climate and Its Variability in CCSM4. *J. Clim.* 1085–1111 (2012). doi:10.1175/jcli-d-11-00326.1
12. Miller, G. H. *et al.* Abrupt onset of the Little Ice Age triggered by volcanism and sustained by sea-ice/ocean feedbacks. *Geophys. Res. Lett.* 39, L02708 (2012).
13. Hatun, H., Sando, A. B., Drange, H., Hansen, B. & Valdimarsson, H. Influence of the Atlantic subpolar gyre on the thermohaline circulation. *Science* 309, 1841–1844 (2005).
14. Després, A., Reverdin, G. & d’ Ovidio, F. Mechanisms and spatial variability of meso scale frontogenesis in the northwestern subpolar gyre. *Ocean Model.* 39, 97–113 (2011).
15. Hurrell, J. W. Decadal Trends in the North Atlantic Oscillation: Regional Temperatures and Precipitation. *Science* 269, 676–679 (1995).
16. Häkkinen, S., Rhines, P. B. & Worthen, D. L. Atmospheric Blocking and Atlantic Multidecadal Ocean Variability. *Science* 334, 655–659 (2011).
17. Condron, A. & Renfrew, I. A. The impact of polar mesoscale storms on northeast Atlantic Ocean circulation. *Nat. Geosci* 6, 34–37 (2013).
18. Langehaug, H. R., Medhaug, I., Eldevik, T. & Otterå, O. H. Arctic/Atlantic Exchanges via the Subpolar Gyre*. *J. Clim.* 25, 2421–2439 (2012).
19. Shabbar, A., Huang, J. P. & Higuchi, K. The relationship between the wintertime North Atlantic Oscillation and blocking episodes in the North Atlantic. *Int. J. Climatol.* 21, 355–369 (2001).
20. Luterbacher, J. *et al.* Reconstruction of sea level pressure fields over the Eastern North Atlantic and Europe back to 1500. *Clim. Dyn.* 18, 545–561 (2002).
21. Gray, L. J. *et al.* SOLAR INFLUENCES ON CLIMATE. *Rev. Geophys.* 48, RG4001 (2010).
22. Woollings, T., Lockwood, M., Masato, G., Bell, C. & Gray, L. Enhanced signature of solar variability in Eurasian winter climate. *Geophys. Res. Lett.* 37, L20805 (2010).

23. Barriopedro, D., García-Herrera, R. & Huth, R. Solar modulation of Northern Hemisphere winter blocking. *J. Geophys. Res.* 113, D14118 (2008).
24. Lockwood, M., Harrison, R. G., Woollings, T. & Solanki, S. K. Are cold winters in Europe associated with low solar activity? *Environ. Res. Lett.* 5, 024001 (2010).
25. Shindell, D. T., Schmidt, G. A., Mann, M. E., Rind, D. & Waple, A. Solar forcing of regional climate change during the Maunder Minimum. *Science* 294, 2149–2152 (2001).
26. Ineson, S. *et al.* Solar forcing of winter climate variability in the Northern Hemisphere. *Nat. Geosci* 4, 753–757 (2011).
27. De Jager, C. & Duhau, S. Forecasting the parameters of sunspot cycle 24 and beyond. *J. Atmospheric Sol.-Terr. Phys.* 71, 239–245 (2009).
28. Barker, S., Greaves, M. & Elderfield, H. A study of cleaning procedures used for foraminiferal Mg/Ca paleothermometry. *Geochem. Geophys. Geosystems* 4, 8407 (2003).
29. Donlon, C. J. *et al.* The Operational Sea Surface Temperature and Sea Ice Analysis (OSTIA) system. *Remote Sens. Environ.* 116, 140–158 (2012).
30. Gao, C., Oman, L., Robock, A. & Stenchikov, G. L. Atmospheric volcanic loading derived from bipolar ice cores: Accounting for the spatial distribution of volcanic deposition. *J. Geophys. Res. Atmospheres* 112, D23111 (2007).



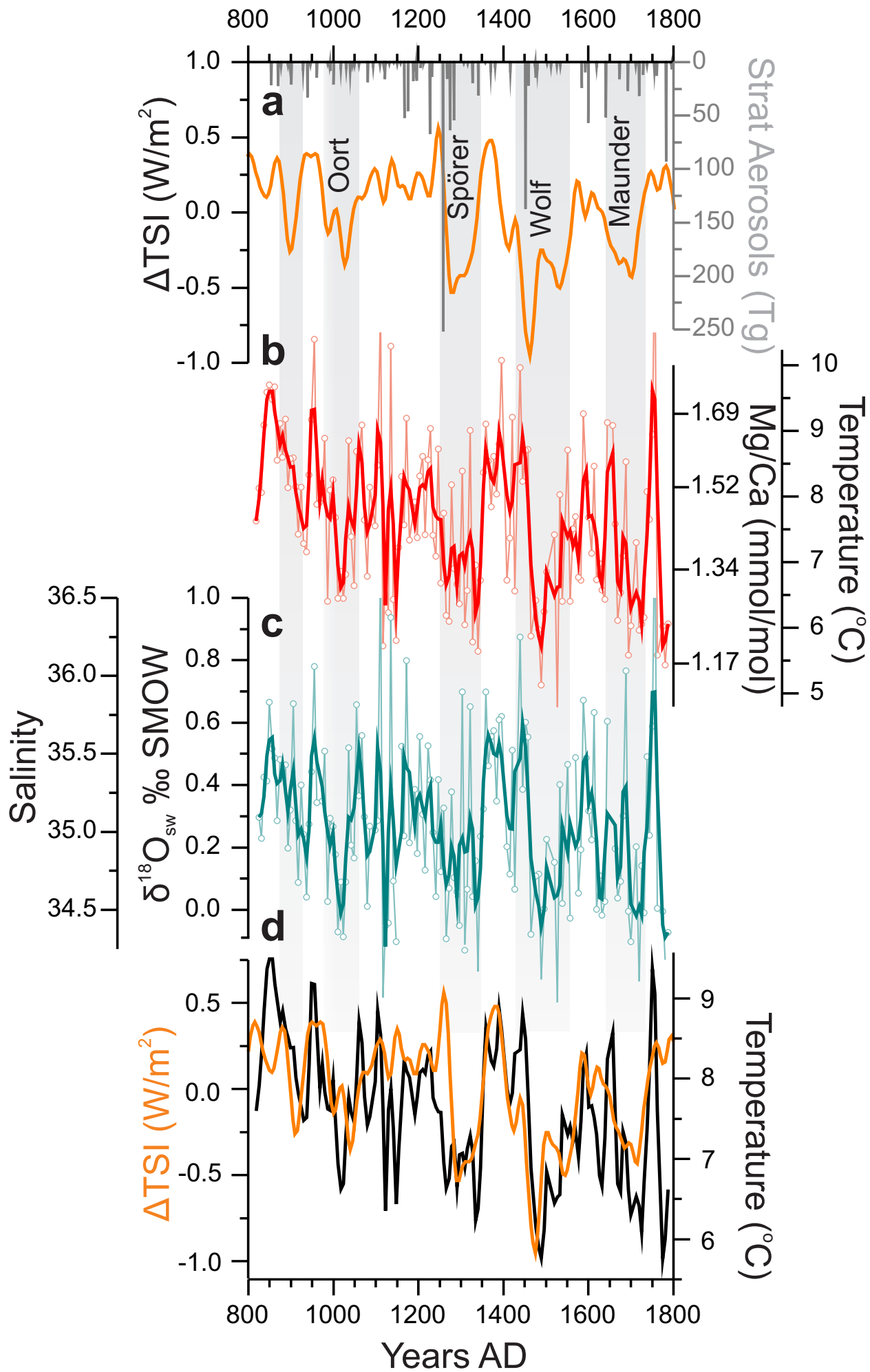


Figure 3.

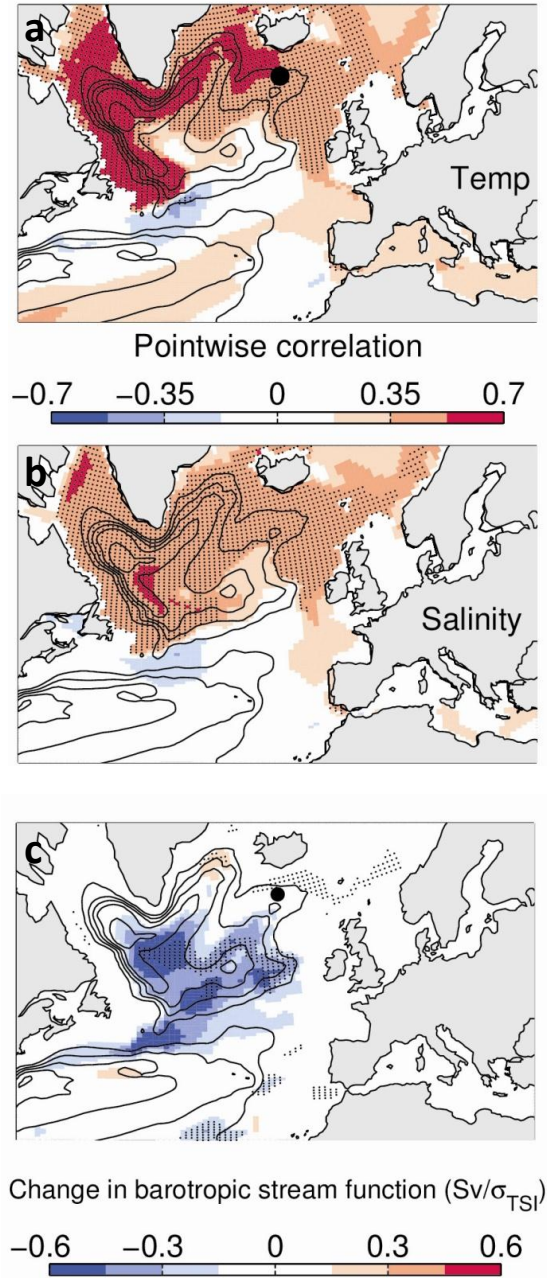


Figure 4.

